Analyst

Accepted Manuscript

ROYAL SOCIETY OF CHEMISTRY

www.rsc.org/analyst

Analyst

RSCPublishing

ARTICLE

Performance Metrics based on Signal Intensity for Ion Mobility Spectrometry - Based Trace Explosives Detectors using Inkjet Printed Materials

J. R. Verkouteren,*[a] J. Lawrence,[a] G. A. Klouda,[a] M. Najarro,[a] J. Grandner,[a] R. M. Verkouteren,[a] and S. J. York[b]

Cite this: DOI: 10.1039/xoxxoooooox

Received ooth January 2012,
Accepted ooth January 2012

DOI: 10.1039/xoxxoooooox

www.rsc.org/

Commercial off-the-shelf (COTS) explosive trace detectors (ETDs) have become an integral part of security practices aimed at protecting the public, transportation, and facilities. Despite their widespread deployment, quality control procedures that can evaluate day-to-day instrument performance or differences among units of the same manufacture are in need of development. In this work, we describe the preparation of test materials (TMs) using inkjet printing that have fixed dosing levels of two explosives; 1,3,5-trinitroperhydro-1,3,5-triazine (RDX) and pentaerythritol tetranitrate (PETN) . The uncertainty in the mass of dispensed solute is 0.8 % (nominal 1 ng RDX and 5 ng or 20 ng PETN depending on ETD). TMs are stable under storage for at least 20 days at temperatures consistent with indoor and outdoor environments, and can be used by field personnel at deployed locations. Inkjet printing is shown to provide the necessary control over the spatial distribution of analyte on the substrate, thus limiting the variability in signal response due to the sample. Measurements of signal intensities for two COTS ETDs were obtained from TMs over multi-year time spans and for multiple units of each ETD. Reproducibility in signal response is shown to be between 6 % and 15 % RSD, or approximately double the within-day variability. The large datasets allow for first time modeling of signal intensities with respect to normal distributions, which supports the use of standard 3-sigma control practices.

INTRODUCTION

Screening technologies that detect traces of explosives are an effective tool against terrorism and are widely used by federal, state, and local agencies tasked with protecting the public. The majority of currently deployed explosive trace detectors (ETDs) utilize thermal desorption for converting collected solid particles to vapor followed by ion mobility spectrometry (IMS) for detection. Commercial off-the-shelf (COTS) ETDs are designed to alarm for selected explosive (or other contraband) threats when the signal response exceeds pre-set threshold levels. Alarm threshold levels are customer- and application-specific, and must balance signal-to-noise requirements with the need to minimize false positives in the varied environments in which the ETD must perform. Quantitative performance of IMS is, in general, considered problematic due to the limited reactant ion concentration resulting from atmospheric pressure chemical ionization (APCI) processes, and the inherent competition for charge among multiple molecular species.[1-2] These limitations have been mitigated to a large degree in research-grade ion mobility spectrometers, but still exist for the COTS ETDs sold for explosives and narcotics detection. As a result, tests of instrument performance of COTS ETDs have primarily been based on the presence or absence of alarms at fixed dosing levels,[3] and vendor-supplied samples contain selected explosives at loadings well in excess of alarm threshold levels.

Tests based simply on alarm status do not provide information on day-to-day performance of the unit or how a unit may compare against others of the same manufacture. These are significant issues to the agencies deploying the estimated 15,000 ETDs that are currently in service.[4] In particular, deployed ETDs are subject to environmental chemical challenges that may be introduced by the collection of samples from surfaces, which, most commonly, involves physical wiping using a collection cloth, or by the introduction of ambient air during thermal desorption and vapor transport. Molecular sieves or chemical desiccants are used to purify air at the inlet, but they are not designed to remove all possible contaminants. The high dosing levels present on vendor-supplied materials may obscure ionization losses that can affect detection near alarm threshold levels. Contaminants may also affect mobility drift times, and standards to address this issue are an active area of research.[5-6] In addition to day-to-day variability

caused by changing environmental and sampling conditions, there may be differences in response behaviours among units from variations in manufacturing. Subtle physical differences in the ion source may affect the number of ions produced, while variations in tube manufacture, electronics, and flow control may affect the transmission of the ions and subsequent amplification of the signal at the detector. The instrument manufacturers have quality control procedures that keep variations within boundaries, but the magnitude of variations in ion signal due to manufacturing uncertainties has not been reported.

These types of evaluations are best accomplished by using numerical measures of the signal response, rather than simple (yes/no) alarm status. The signal intensity to a fixed dosing level provides access to standard quality control approaches, and allows for more robust prediction of expected responses with respect to alarm threshold levels. In a study of methamphetamine remediation practices, the IMS signal intensity for this compound was found to vary significantly by operator and date over a two week period.[7] In this case, the test samples were prepared by pipetting by each operator, and differences in sample preparation may have contributed to the variability. Samples are introduced to COTS ETDs on the substrates used to collect them; these substrates become part of the sample in the thermal desorption process and must be considered as sources of contamination. Additional requirements exist for placement of the analyte on the substrate because of the design constraints of thermal desorbers. There are also choices for the specific metric to use for signal intensity, particularly for explosive compounds, as more than one adduct may be produced for each compound. Finally, the ion signal is heavily processed by the resident software in ETDs, and measurements of intrinsic background are difficult to obtain. Truncated data, where the peak intensities are not continuous from zero, impact estimation of the limit of detection (LOD), which has recently been addressed by a standard test method in ASTM.[8]

In this work, we present the first evaluations of ETD signal intensity measured for the same dosing levels over multi-year time spans and across multiple units. For this purpose, we developed test materials (TMs) containing single dosing levels of 1,3,5-trinitroperhydro-1,3,5-triazine (RDX) and pentaerythritol tetranitrate (PETN) using inkjet printing technology. The dosing levels are well above the LOD to avoid issues with peak intensities near background levels. The utility of inkjet printing for production of test materials has been demonstrated,[9] and here we evaluate the factors that must be controlled to minimize instrument response variability arising from the sample. Measurements of signal intensity are shown to provide a mechanism for quality control of individual units, and to provide measures of comparison among units. The large datasets allow for first time modeling of the intensity distributions, which establishes the framework for robust prediction of ETD response for a single sample at a known dosing level and across multiple units.

EXPERIMENTAL

IMS Instrumentation and Data

Two types of commercial off-the-shelf (COTS) ETDs were used in this study, and we refer to them simply as ETD 1 and ETD 2. Eighteen different instruments were evaluated, including one laboratory-based instrument each of ETDs 1 and 2, one field-deployed unit of ETD 2, and 15 field-deployed units of ETD 1. The field-deployed unit of ETD 2 is on the NIST campus, and the 15 field-deployed units of ETD 1 are distributed among 9 different countries with very different outdoor environmental conditions. The field deployed units (non-aviation based) are all housed in enclosures that have varying degrees of exposure to the outside, and are used for screening activities. All units were operated under the general conditions listed in Table 1.

Table 1. Operational parameters for COTS ETDs

IMS Operation Parameter	ETD 1	ETD 2
Desorber Temperature (°C)	220	205
Detector or Tube Temperature (°C)	163	109
Drift flow (cm^3/min)	100	300
Sample flow (cm^3/min)	50	550
Sampling time (s)	8	5

It must be noted that each ETD manufacturer has developed proprietary system firmware for digital processing of raw signals. The signal intensities reported from the COTS ETDs studied here are background-corrected maximum signal amplitudes achieved during thermal desorption in particular channels as identified through the firmware. The proprietary nature and efficacy of the digital processing are unimportant to this study since our intention is to report performance metrics of the COTS systems as distributed, as observed through the use of the inkjet-based test materials.

The ion chemistries for RDX and PETN in ETD 1 have been described in Kozole et al.[10] and example spectra in negative ion mode obtained from one instrument are shown in Figure 1. Before sampling begins, the spectrum contains the mobility peak for the reactant ion (RIP), which is produced by interaction of ^{63}Ni with dichloromethane-doped purified air, and is identified in Kozole et al.[10] as $Cl^- \cdot xH_2O$. Intensities are given in digital units (du). During sampling the RIP intensity decreases as product ions are formed. Only the moderate to major intensity product ions from Kozole et al. are shown in Figure 1, but they also correspond with instrument detection channels. The two primary product ions of RDX are not resolved, but for these samples the chloride adduct is dominant with the tail of the peak in the detection channel for the nitrate adduct. PETN produces a minor to major intensity $[NO_3]^-$ peak by decomposition that corresponds to a detection channel; the peak is not selective for PETN and was not included in the analysis. The RIP was included in the analysis; this

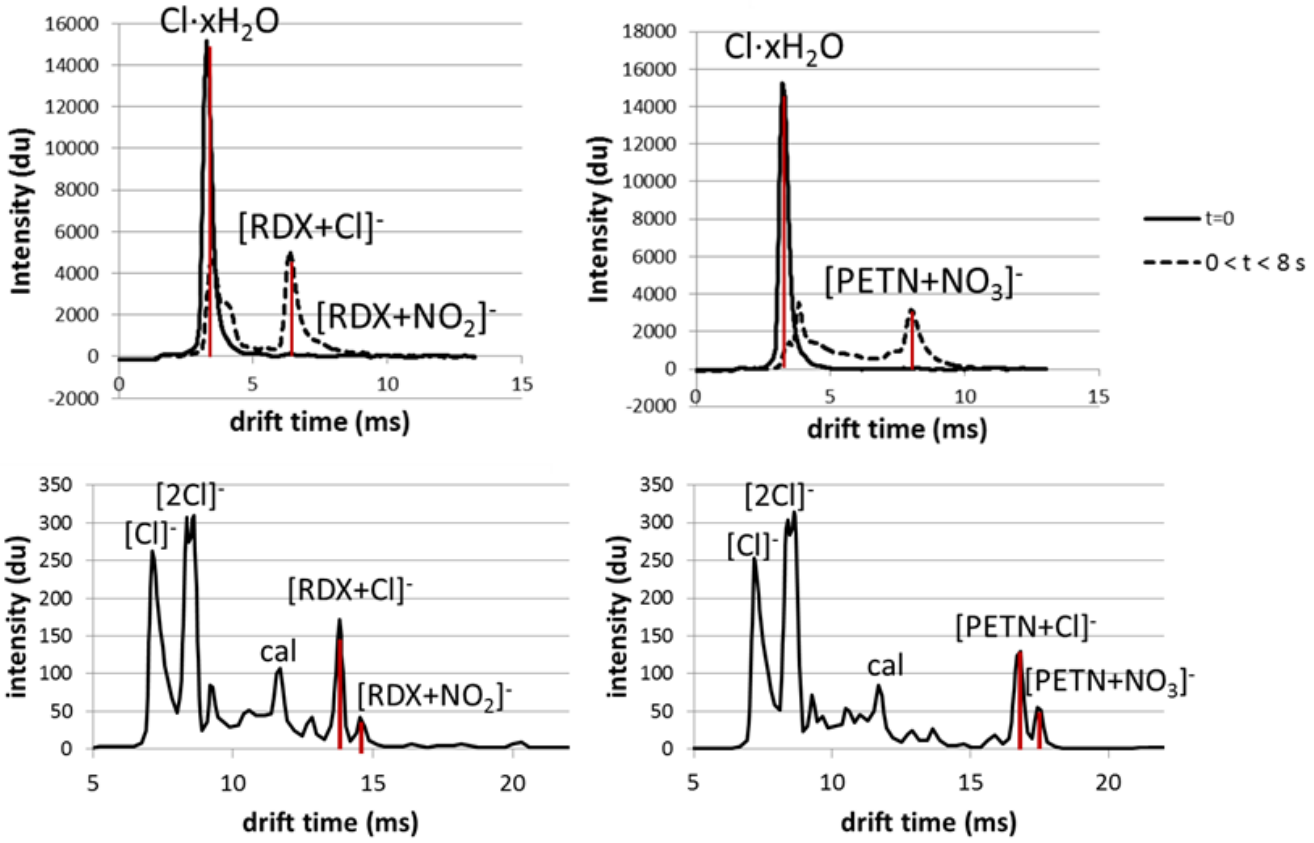

Figure 1. Example IMS spectra for ETD 1 (top) and ETD 2 (bottom) with peak identifications from references 10 and 11.

peak is almost always the most intense peak in the plasmagram and has drift times that range from 3.2 ms to 3.4 ms.

The ion chemistries for RDX and PETN in ETD 2 are similar to ETD 1 and have been described in Kozole et al.[11] with example spectra given in Figure 1. The RIP for this instrument arises from hexachloroethane and comprises two peaks, $[Cl]^-$ and $[2Cl]^-$. The intensities of these peaks were found to provide little information, as opposed to ETD 1, and were not used in this analysis. There is an additional background peak for 4-nitrobenzonitrile which is the internal mobility drift time calibrant. The chloride monomer adduct is present for PETN in ETD 2 and resolved from $[PETN+NO_3]^-$; the sum of these two peaks is used for PETN. The two primary adducts of RDX are resolved in ETD 2, and the sum of the two intensities is used. A low intensity peak for the chloride dimer adduct of RDX is observed at approximately 20 ms in some spectra, but was not used for analysis. The formation of dimer relative to monomer is favoredwith increasing analyte concentration in IMS,[2] and for these samples, the loading amount is sufficiently low that the dimer intensity is near background levels.

Inkjet Printing of Test Materials (TMs)

TMs are prepared by dispensing explosives solutions onto ETD-specific substrates using drop-on-demand inkjet chemical printing. The substrates are woven PTFE-coated fiberglass (manufacturer supplied) for ETD 1 and woven meta-aramid fiber (manufacturer supplied) for ETD 2 and have physical dimensions that allow for insertion into the thermal desorber slot located on the front of each ETD. The substrates are placed on custom-designed trays (Figure 2) to allow for precise placement of solution.

The piezoelectric inkjet printer (Jetlab 4 XL-B, MicroFab Technologies, Inc., Plano, TX)† has an integrated microbalance (SE2-F, Sartorius Group, Bohemia, NY) for measurement of droplet size and a pressure/vacuum regulator (PC90, MKS Instruments, Andover MA) coupled to a differential pressure transducer (MKS698A) to control headspace pressure in the fluid reservoir. Droplets are dispensed on-demand from devices with nominal 50 µm orifices in discrete bursts ranging from 1 to 999 drops.

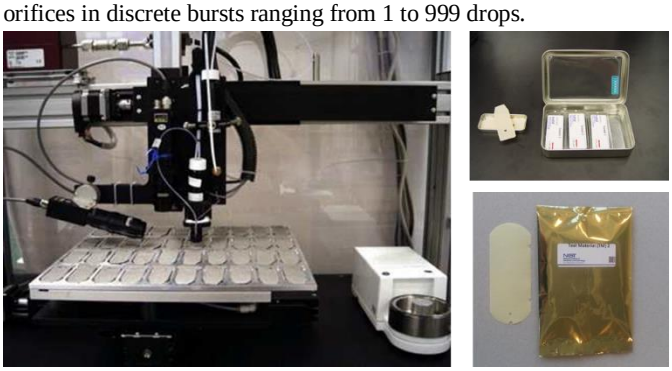

Figure 2. Inkjet printing of solutions on substrates held in customized trays (left) and prepared TMs for ETDs 1 and 2.

Table 2. TM production parameters based on 40 ng drop size and 100 mg/L solution concentrations.

	ETD 1		ETD 2	
	RDX	PETN	RDX	PETN
Target loading*	1 ng	20 ng	1 ng	5 ng
Droplets/burst	196	246	196	246
Burst array	single spot	4 by 4†	single spot	2 by 2‡
Volume dispensed	10 nL	200 nL	10 nL	50 nL

*Determined from measured instrument response curves to be well above detection limits.
†X and Y spacings of 0.7 mm
‡X and Y spacings of 1.7 mm

Depending on the targeted loading mass, drops are dispensed in single bursts or in arrays of bursts (Table 2). The loading mass is selected to be well above the detection limit, and fully desorbed in the ETD in a single analysis. The driving waveform has a pulse height of 32 V, pulse width of 30 µs, and rise and fall times of 4 µs each. The values for the waveform are adjusted as needed to address daily differences in droplet formation resulting from subtle changes in orifice condition. Droplets are ejected at 500 Hz and the fluidic pressure is maintained slightly negative relative to atmospheric pressure.

The spatial location of the sample on the substrate is critical for COTS ETDs due to the limited desorber area relative to the size of the substrate. In both cases, the desorber is accessed from an open slot in the front of the ETD, and the substrate must be considerably longer than the desorption region to allow for insertion and removal. The heated area of the substrate is dependent on the physical dimensions of the desorber and the reproducibility in placement of the substrate. Within the heated area, there may be differences in the efficiencies of vapor transport to the inlet,[12] resulting in differences in signal intensity. To determine optimal printing locations based on signal intensity, RDX and PETN were deposited along x and y traverses at 3 to 5 mm intervals. The leading edges for both substrates for insertion into the desorber is at x = 0. Three replicates were printed at each location, and the average intensities relative to the maximum are shown in Figure 3.

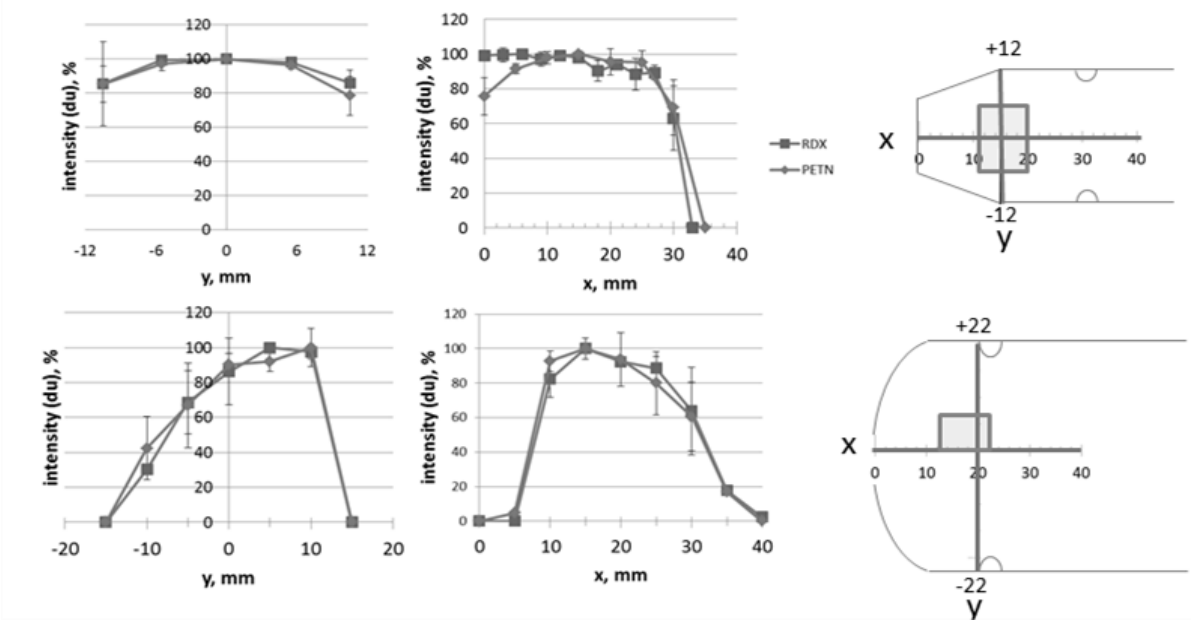

Figure 3. Intensity variations with position on substrate for RDX and PETN for ETD 1 and ETD 2. Targeted printing regions for TM production given by shaded boxes.

For ETD 1, the RDX signal is relatively constant from the leading edge to x = 25 mm, falling to zero at x = 35 mm. The PETN signal is at its highest between 10 mm and 25 mm in x. The decrease in PETN near the leading edge is consistent with a higher temperature at this location, as PETN intensities are typically optimized at lower desorber temperatures compared with RDX.[13] The desorber is open to the atmosphere so temperature heterogeneities would be expected. For both analytes, the signal response is symmetrical in y with the lowest values at the edges of the substrate. The printing region, taking into account uncertainties in stage motion and substrate placement on the printing trays, is a 10 mm by 16 mm area shown by the shaded box.

For ETD 2, the RDX and PETN signals are both at their highest between 10 mm and 25 mm in x, and between 0 mm and +10 mm in y. The asymmetry in the y traverse may be due to inefficiencies in vapor collection, as this ETD has two drift tubes to allow for simultaneous detection of positive and negative ions, and requires a split in the air flow from the desorber. The negative ion drift tube is on the right side of the split, corresponding to the favored location on the substrate. The printing region shown by the shaded box is 10 mm by 8 mm.

Solution Preparation

Solutions are prepared gravimetrically using crystalline RDX or PETN (Cerilliant, Round Rock, TX) with stated purity factors of 99.8 % ± 0.39 % for RDX and 99.3 % ± 0.39 % for PETN (uncertainties given as 95 % confidence intervals with k = 2). Milligrams of crystalline material are weighed (AT21 comparator balance, readability 1 µg, Mettler Toledo, Columbus, OH) into preweighed quartz boats and the solvent (2-propanol, HPLC grade) is weighed (Mettler ATIC balance, readability 10 µg) into 50 mL volumetric flasks. A minimum of five replicate mass measurements of each value are obtained, the container weights are subtracted, and the averages and standard uncertainties calculated. Solvation occurs after a few hours facilitated by stirring and ultrasonic agitation; the latter limited to 15 min between stirring. Solution concentrations are nominally 100 mg/L, which are well below saturation concentrations for each explosive. From the mass of the solute (m_{s1}) and the solvent (m_{s2}), and the solute purity (p), the mass fraction: $p * (m_{s1}/(m_{s1} + m_{s2}))$, and its combined uncertainty are calculated for k = 2 using GUM[14] and Ku[15] (Table 3). The equivalent concentration and uncertainty in µg/mL are calculated assuming the density of 2-propanol to be 0.786 g/mL at 20 °C. A 2-mL aliquot of solution is transferred to amber ampoules, hermetically sealed in an argon atmosphere, and stored under refrigeration until use.

Evaluation of Uncertainty

A comprehensive evaluation of total uncertainty in TM preparation was performed according to standard guidelines.[14-16] Table 3 lists all factors and error sources considered, with a discussion of the uncertainty in the solute concentration given in the previous section. While commercially available, systems capable of chemical printing are not widely distributed and standard methods for these depositions have yet to be developed. We have, however, verified the deposition process through refereed methods, including UV-vis, GC-MS and HPLC, by printing directly into sampling vials. The gravimetric method used for estimating the mass of solution dispensed has been carefully designed to avoid deleterious effects from droplet evaporation, changes in orifice wetting from crust formation, static charge, magnetism, air buoyancy, and first drop issues (missing or variable-size drops).[17] A critical aspect is using the same number of droplets per burst during the gravimetric characterization and the TM deposition.[18] The uncertainty in the mass of solution dispensed may be estimated by considering three sources of error: balance calibration, algorithm fit, and measurement imprecision. The first is the error possible from non-linear deviations in the calibrated response of the microbalance. The gravimetric method utilizes differential, not absolute, mass measurements amounting to about 800 µg, and linearity errors are reported to be less than 0.9 µg by the balance manufacturer. This error is therefore estimated at 0.11 %. The second source of error, algorithm fit, is estimated by the difference in output between two disparate evaporation models used to calculate droplet burst mass. The third source of error is the

Table 3. Uncertainty budget for inkjet-printed TMs.

Factor	Error Source	Expanded uncertainty k = 2	Combined uncertainty
Mass of solution dispensed	Balance calibration	0.1 %	0.6 %
	Algorithm fit	0.2 %	
	Measurement imprecision	0.6 %	
Solute concentration	Impurity of solute	0.4 %	0.4 %
	Gravimetric preparation	0.1 %	
Total combined expanded uncertainty of dispensed solute			0.8 %

observed variation in output from repeated gravimetric analyses. Control over the fluidic pressure to ± 0.02 hPa allows for long-term stability in droplet mass dispensed over the time period required for preparation of multiple trays of TMs, with estimated expanded uncertainties of 0.6 %. [The measurement imprecision may be dependent on factors such as the solvent and the number of droplets in a burst, and the values in Table 3 are specifically for generation of TMs and not generalized for inkjet printing.] Expanded uncertainties are combined in quadrature for a total combined expanded uncertainty in dispensed solute for TMs of 0.8 %.

Storage

The small solution volumes used for TM production allow for rapid drying, and samples are ready for packaging immediately following printing. TMs were packaged for ETD 1 in sets of 5 in slide-top tin containers (79 mm x 35 mm x 10 mm). TMs were packaged for ETD2 in sets of 5 in heat-sealable metallized bags that are purged, backfilled with N_2, and sealed (AccVacs T1500G vacuum sealer, Henderson, NV). The TMs are encased in an aluminium foil sleeve within the bag to protect them from contact with the linear low-density polyethylene lining of the bag. Samples were stored under laboratory conditions (20 ± 2 °C, 45 ± 10 % RH) or, for testing purposes, in an environmental chamber (LH series, Associated Environmental Systems, Ayer, MA) at 32 °C, 75 % RH. The temperature and humidity uncertainties in the environmental chamber as reported by the manufacturer are ± 0.5 °C and ± 2 % RH at the sensor, respectively. For TMs shipped to deployed locations (ETD 1 only), individual tins were packaged together in a larger tin with a non-reversible temperature indicator (Thermax 6-level strip, 29 °C to 42 °C) attached to the lid. The temperature indicator was used to document the highest temperature experienced from shipping to analysis.

RESULTS

Laboratory Units

TMs were analysed on ETD 1 and ETD 2 for over two years, and the data are shown in Figures 4 and 5. This time span also included continued research and testing of different TM formulations, and a fixed schedule of testing was not established resulting in time gaps. The variability within a day ($n \geq 3$) averaged between 4 % and 6 % RSD for both analytes on both ETDs, and the variability across the

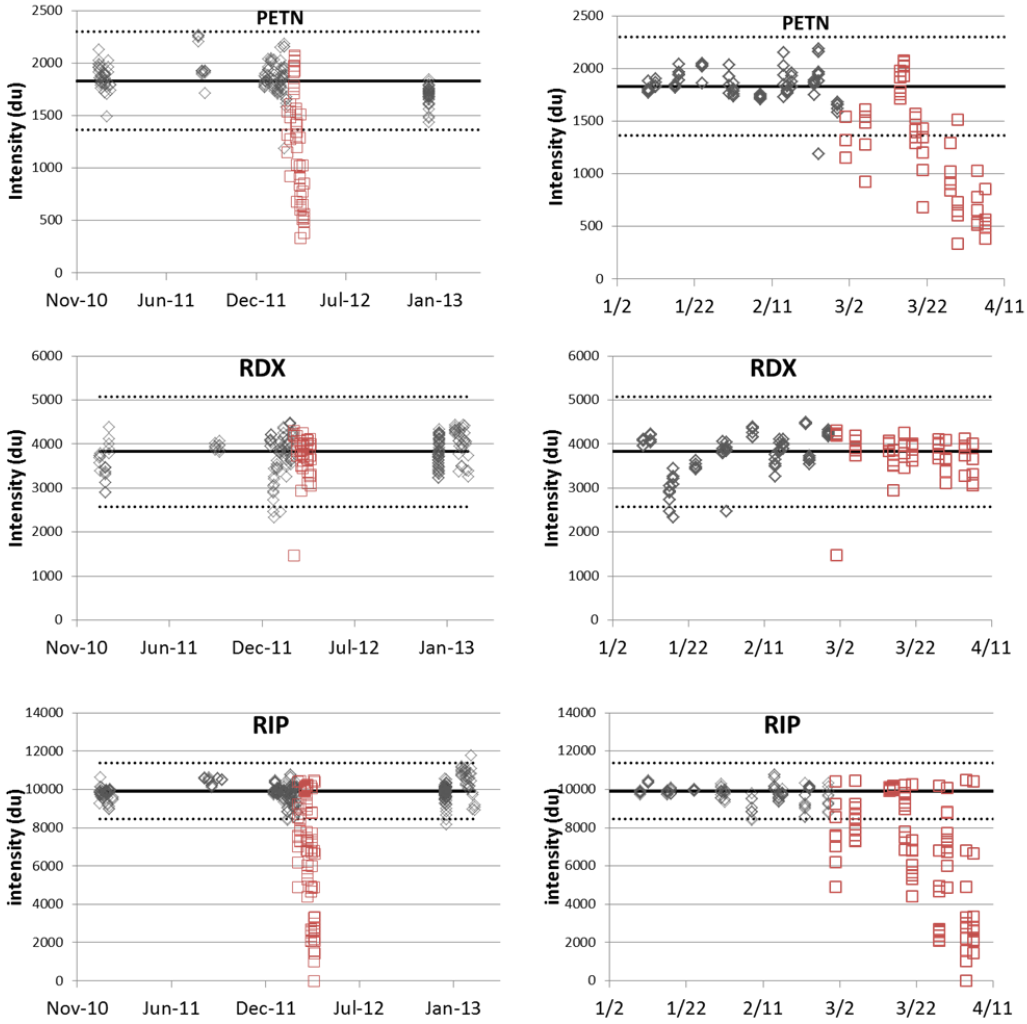

Figure 4. Intensity data from TMs for laboratory based COTS ETD 1 from 1/2011 to 2/2013 with average (solid line) and UCL and LCL (dotted lines). Selected time frame shown in more detail on right. Data in red squares removed prior to calculation of statistics.

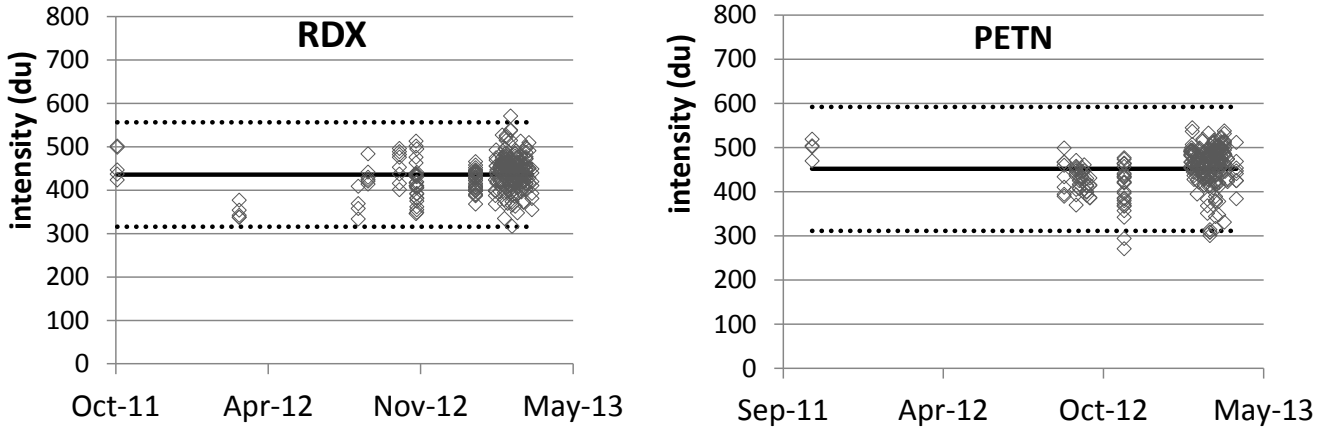

Figure 5. Intensity data from TMs for laboratory based COTS ETD 2 from 10/2011 to 4/2013 with means (solid line) and UCL/LCL (dotted lines).

entire study period is approximately double that amount (Table 4). The daily variability is comparable to that observed for differences in sample location of a few millimetres, and is therefore near a minimum value for these types of instruments. The average response is represented as the center line in Figures 4 and 5, and upper and lower control limits (UCL and LCL, respectively) were calculated based on "3-sigma" standard practices.[19] The sample standard deviation (SD) is considered a biased estimator of σ and is typically corrected for n < 25 by multiplying by a factor (C_4) that is based on sample size. The samples sizes for our data all exceed 25 and C_4 ranges from 0.9972 (n = 90) to 0.9994 (n = 363), so that corrections to the standard deviation are within rounding error of the values reported in Table 4.

The data collected for ETD 1 from 3/1/2012 to 4/6/2012 (shown in red in Figure 4) were excluded in the calculations given in Table 4 because they were deemed to be out of control. The signal intensities of the RIP and PETN deteriorate significantly during this time period, with decreasing average values and an increase in the daily variability (22 % RSD for PETN and 32 % RSD for the RIP). The signal intensity of RDX does not show a comparable decrease, but the variability over this time frame is higher than average (daily RSD of 10 %). Both ETDs were maintained over the study period following manufacturer's specifications, and always indicated a ready state prior to testing. Analysis of TMs, therefore, provided unique information about the performance of ETD 1 and unambiguously indicated a negative change. Both ETDs were used during the study period for other research activities, and it is likely that a contaminant was introduced to ETD 1 that affected the RIP intensity and consequently, the PETN intensity. The unit was taken offline and serviced, and subsequent testing with TMs showed a return to control levels for all 3 signal intensities.

ETD 2 did not exhibit a similar deviation from control over the two year study period, but it did exhibit warm up issues indicated by low intensities for the first few samples of the day for each analyte. Explosive compounds are known to have a propensity to adsorb on surfaces in the ETD resulting in loss in ion signal.[20] The solution for the lab instrument was conditioning with 2 to 3 TMs each of PETN and RDX prior to recording data. For field instruments, the use of heavily loaded calibrant samples during the start-up routine accomplishes the same task. We did not observe the same warm up issues with the deployed unit of ETD 2 included in this study.

The data collected for both ETDs were also evaluated by generating histograms to model the distributions of intensities (Figures 6 and 7). There is no expectation based on the literature for the form of the distribution, and we started with the simplest model of a 3 parameter Gaussian. The overlays of the fitted distributions indicate that the assumption of a normal distribution is not unreasonable. The correlation coefficient (R^2) is 0.94 or higher for RDX and PETN for both laboratory ETDs (Table 4). The RIP intensities (ETD 1) have considerably larger tails than expected, and this is reflected in the relatively low R^2 of 0.91 and the factor of 2 difference in the estimate of dispersion based on the arithmetic calculation compared with the fitted value. The RDX distribution from ETD 1 is truncated on the high intensity side, which is consistent with the intrinsic limitation imposed on the chloride adduct intensity by the availability of reactant ion peak. PETN in ETD 1 is limited by decomposition to form $[NO_3]^-$, and the $[PETN+NO_3]^-$ peak intensity does not exhibit the same truncation.

The distributions for ETD 2 are also well approximated by a Gaussian, which is interesting given the fact that they are sums of two adducts that, in themselves, have skewed distributions. The distributions of the chloride (C) adduct of both RDX and PETN are

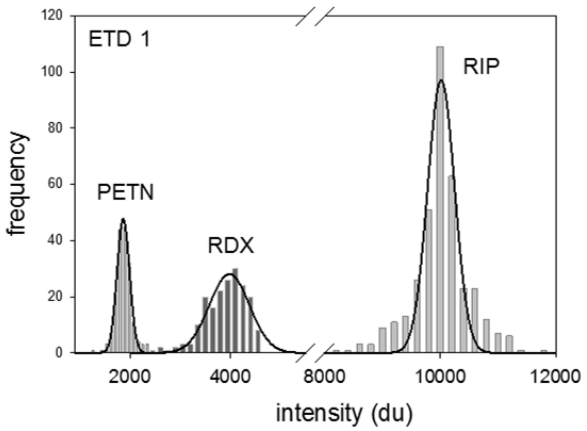

Figure 6. Histograms of intensity data from TMs for laboratory based COTS ETD 1.

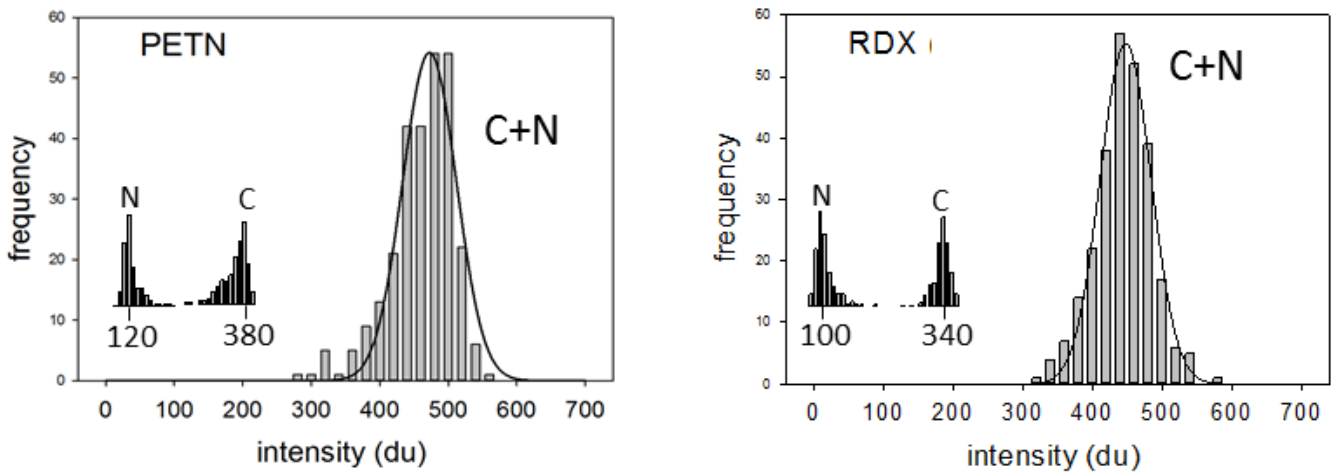

Figure 7. Histograms of intensity data from TMs for laboratory based COTS ETD 2.

skewed low, whereas the nitro and nitrate (N) adduct distributions are skewed high. The PETN C + N distribution exhibits a slight skew to lower intensities, but more data would be required to determine if this is a significant deviation from normality. The variability in the individual product ions is most likely a function of changing background levels of nitrate, with varying contributions from the substrate or ambient air. The substrate used for ETD 2 must be treated by the ETD manufacturer to reduce background contamination, and there can be differences in C/N ratios according to purchased lot number. A paired study (n = 18 each) of two different lots of substrate showed that even though the C/N ratios for PETN were significantly different (p = 5E-04), the sums were not (p = 0.12). The data suggest that the reaction rates favouring one product ion over another may vary, but that total ion production is conserved.

Storage

The stability of the TMs under storage was tested by evaluating signal responses immediately after printing (time = 0 in Figure 8) and then periodically for 30 days. When held under laboratory conditions, no trend in signal response with storage time was observed for the 4 TMs for the specific batches shown in Figure 8. We have observed some instability for the RDX TM for ETD 1 for different printed batches, and it may be due to subtle differences in surface chemistry of the substrate from lot to lot. For this particular TM, we periodically check the stability of printed batches and prefer to limit the storage to 20 days or less, if possible. The other three TMs have shown no signs of instability, and they can be stored for at least 30 days prior to use.

Storage was also evaluated at elevated temperatures to account for field deployment conditions. The TMs for ETD 2, which were stored in sealed, metallized bags, did not degrade when held at 32 °C, 75 % RH for 30 days. A paired study of samples held for 30 days at the two temperatures showed no difference in signal intensity for PETN (n = 40, p = 0.37) and a slight increase (4 %) for RDX at elevated temperature (n = 40, p = 0.04). If the TMs are not stored in sealed bags, there is degradation in signal intensity for samples held at the higher temperatures, with a 10 % decrease for PETN (n = 40, p = 1E-05) and an 18 % decrease for RDX (n = 40, p = 3E-11). The TMs for ETD 1 could not be stored in sealed bags, even under laboratory environmental conditions, because of induced chemical changes that cause the mobility drift times of RDX and PETN to shift from the detection windows.[21] In the unsealed tins, the PETN TM for ETD 1 showed no loss in signal intensity for 30 days at 32 °C, 75 % RH, whereas the RDX TM exhibited degradation in signal intensity over room temperature storage.

Deployed (non-aviation based) Units

NIST has two ETDs deployed for screening purposes which were available for long term evaluation with TMs. The deployed unit of ETD 1 is used to screen incoming packages and vehicles, and is housed in a loading dock that is frequently open to the outside. The unit was purchased new and evaluated upon receipt and then for four months under deployed conditions. The deployed unit of ETD 2 is used to screen incoming vehicles, and is housed outside in a small enclosure. This unit had been in service for approximately 1 year prior to evaluation. The deployed unit of ETD 1 is significantly different in performance compared to the laboratory unit. All three signal intensities are lower for the deployed unit, with a difference of (–) 46 % for the RIP, (–) 40 % for RDX, and (–) 13 % for PETN. This is due primarily to inherent differences in manufacture, as the average signal intensities measured upon receipt and installation of the instrument were close to the values reported in Table 4. The RDX signal intensity was initially 2738 du (n = 8, SD = 47 du), the PETN intensity was 1692 du (n = 9, SD = 18 du), and the RIP intensity is unchanged. The dispersion of the data increased during deployment, with daily RSDs increasing from 1 %, 2 %, and 4 % for PETN, RDX, and the RIP, respectively, to the higher values shown in Table 4. This increase in variability may be due to general use of the ETD, rather than any specific environmental contamination. There was no correlation in signal intensities with respect to daily temperature or humidity conditions recorded near the unit.

Table 4. Statistical measures of COTS ETD response to inkjet-printed TMs.

		Intensity (du)							
		arithmetic					Gaussian fit*		
signal	n	avg	SD	%RSD	daily %RSD	bin	*x0*	*b*	R^2
ETD 1 Lab Unit (1/2011 to 3/2013, excluding 3/1/1012 to 4/6/2012)									
RIP	363	9918	485	5	2	200	10016	234	0.91
RDX	188	3825	415	11	5	150	3978	400	0.94
PETN	175	1829	156	9	4	90	1863	125	0.99
ETD 1 Deployed Unit (2/2013 to 6/2013)									
RIP	194	5313	469	9	4	100	5407	279	0.90
RDX	104	2295	342	15	8	100	2371	384	0.81
PETN	90	1597	89	6	3	50	1631	87	0.97
ETD 1 all 16 units									
RDX	80	3151	1018	32					
PETN	80	1934	602	31					
ETD 2 Lab Unit (10/2011 to 4/2013)									
RDX	263	435	41	9	6	20	447	37	0.99
PETN	277	452	47	10	6	20	473	39	0.95
ETD 2 Deployed Unit (2/1/2013 to 4/1/2013)									
RDX	106	499	69	14	7	20	536	43	0.86
PETN	112	493	69	14	6	20	528	44	0.90

* $y = ae^{-0.5(\frac{x-x0}{b})^2}$ (the value of a is unimportant and not reported)

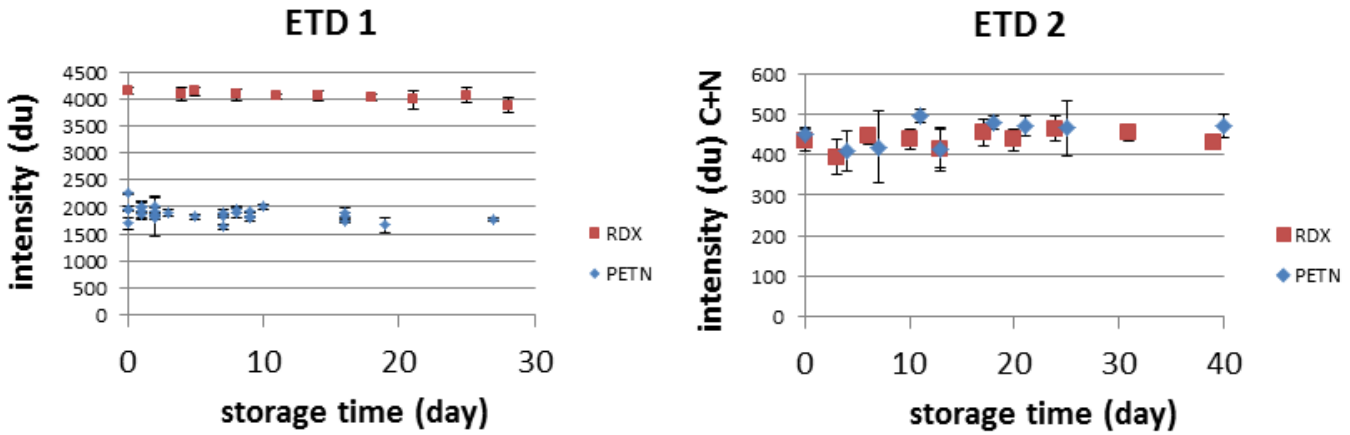

Figure 8. Stability of signal responses from TMs with respect to storage under laboratory conditions (20 ± 2 °C, 45 ± 10 % RH). Error bars represent 1 SD.

The importance of signal intensity arises from the relationship to fixed alarm thresholds, which, for ETD 1, may be 1000 du or 1250 du for RDX, depending on software version. The LCL for the deployed unit is currently 1269 du, and therefore 99.9 % of TM samples should have intensities above alarm thresholds. However, for the same loading amount of RDX, the laboratory unit has a LCL of 2580 du, and could accommodate more deterioration or variability in signal intensity without compromising alarm probabilities. The intensity distribution for the deployed unit is somewhat skewed for RDX, reflecting the decrease in intensity over the study period, but there is no indication of a different underlying distribution of data. Early data that reflects the starting condition of the unit may be removed at some point from the control set, and new limits can be calculated to reflect current conditions. This would raise the LCL of the deployed unit by reducing the variability in the data, but only slightly (1313 du).

The deployed unit of ETD 2 is also significantly different in performance compared to the laboratory unit, although the signal intensities of RDX and PETN are actually higher for the deployed unit. The variability for the deployed unit is larger for both analytes, and the correlation coefficient from the Gaussian fit reflects a larger deviation from normality. The within day variability ($n \geq 3$) is comparable to the laboratory unit, but the day-to-day variability is larger by 30 % to 40 %. As a result, the LCLs for both analytes for the laboratory unit are higher than the corresponding LCLs for the deployed unit. The LCLs (286 du to 312 du) are well above alarm thresholds, although for this ETD the alarms are based on detection of 2 adducts for RDX and PETN. The individual adduct intensities are more different for the two units as compared to the sums (Table 5), and the deployed unit has a higher C/N ratio for both analytes. The results in Table 5 were determined for TMs printed on the same lot of substrate, and therefore the differences in C/N ratio reflect fundamental differences in the units or their ambient environment, and not differences due to substrate. As described earlier, the sum of the adduct peaks exhibits a normal distribution, whereas the individual adduct peak intensities do not, and therefore we use the sum for control chart purposes. We note, however, that the detection threshold for the N adduct is typically 15 du, and LCLs calculated for both analytes would be below this threshold for both units.

A larger sampling of deployed ETD 1 units (16 total) was accomplished by shipping or carrying samples immediately following printing to remote locations for a single day analysis, with 5 replicates of each TM. For TMs that were shipped, non-reversible temperature

Table 5. Comparison of individual adduct intensities for laboratory and deployed units of ETD 2.

	RDX						PETN					
	n	C (du)		N (du)		C/N	n	C (du)		N (du)		C/N
		avg	SD	avg	SD			avg	SD	avg	SD	
lab	54	338	28	91	28	3.7	57	343	68	114	40	3.0
depl.	61	433	69	60	25	7.2	58	444	42	76	21	5.8

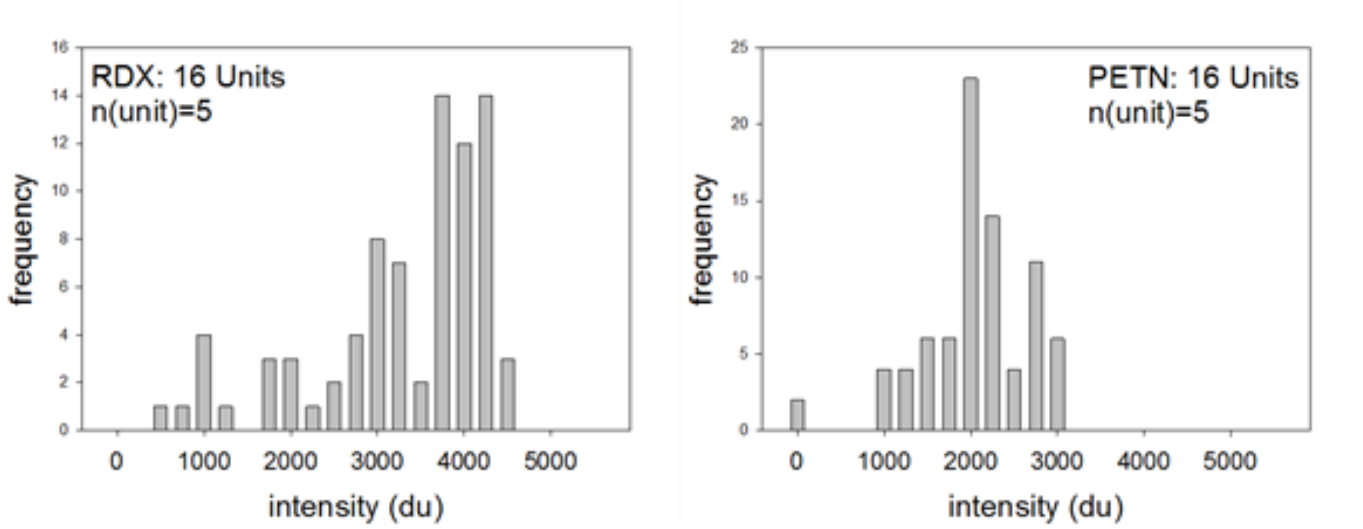

Figure 9. Histograms of intensity data from TMs for 16 units of COTS ETD 1. Bin size 250 du.

indicators included with the shipment indicated, in all cases, that the maximum temperature experienced was lower than 29 °C. These data were binned by intensity (250 du bin size) to generate the frequency histograms shown in Figure 9. The RDX intensity values exhibit a range consistent with the two units evaluated at NIST, with a maximum value of 4500 du and a minimum value of 500 du. The PETN values have a more limited range, also consistent with the two units at NIST, with maximum values of 3000 du and a minimum value of 0 du (non-detect). The variability in the combined data is larger than expected for individual instruments (RSDs of 31 % and 32 %), consistent with real differences among instruments. These data can be expanded to include more instruments and generate expected performance statistics for large numbers of instruments. Those instruments that produce values near the bottom of the distribution, or below alarm thresholds, can be evaluated further to determine whether maintenance or repair might be needed.

Conclusions

We have demonstrated that the signal intensity produced by COTS ETDs can be used to provide robust statistical measures of performance. These performance measures allow for discrimination among units of the same manufacture, evaluation of day-to-day performance, and prediction of expected outcomes with respect to alarm status. The successful use of signal intensity is highly dependent upon a source of well controlled standard test materials. In our case, TMs were produced by inkjet printing, and critical factors under control include the location of the sample on the substrate and the choice of substrate, the composition of the sample, storage mechanisms, and the choice of signal metrics – single *vs* multiple adducts. Signal intensities from analysis of well controlled TMs follow normal distributions, which allows for development of control charts to monitor the performance of COTS ETDs. Three-sigma control limits can effectively describe probabilities of detection for 99.9 % of samples at fixed dosing levels of explosives. The stability of TMs under time frames necessary for shipment and analysis at deployed locations was demonstrated, along with their stability under normal ambient conditions. The samples were run by field personnel, and the data are available directly from the user interface of the two COTS ETDs evaluated in this study. The ease of use allows for application to large numbers of COTS ETDs, which will also provide the underlying data to discriminate underperforming instruments and/or those requiring maintenance. This could provide a mechanism for more nuanced evaluation of large inventories of instruments, and establish metrics by which to judge and improve new trace detection technologies.

We have begun distributing test materials to US agencies under the agreement specified in the acknowledgements for quality control of deployed ETDs. In addition, we have plans for transitioning the production of inkjet printed materials to agencies or companies outside of NIST to meet future demands for wide-scale quality control of ETDs.

Acknowledgements

Portions of this material are based upon work supported by the Science and Technology Directorate of the U.S. Department of Homeland Security under Award numbers HSHQDC-11-X-00420 and HSHQPM-12-X-00070.

Notes and references

[a]National Institute of Standards and Technology (NIST), 100 Bureau Drive, Mailstop 8371, Gaithersburg MD 20899
[b]U.S. Department of State DS/FSE/FSB, 8380 Alban Road SA-18 Rm. 230, Springfield, VA 22150

† Certain commercial equipment, instruments, or materials are identified in this document. Such identification does not imply recommendation or endorsement by the National Institute of Standards and Technology, nor does it imply that the products identified are necessarily the best available for the purpose.

1 C. G. Fraga, D. R. Derr and D. A. Atkinson, Improved quantitative analysis of ion mobility spectrometry by chemometric multivariate calibration, Analyst, 2009, 134, 2329-2337.
2 J. Puton, S. I. Holopainen, M. A. Mäkinen and M. E. T. Sillanpää, Quantitative response of IMS detector for mixtures containing two active components, Anal. Chem. 2012, 84, 9131-9138.
3 ASTM E2520-07, Standard Practice to Verify Minimum Acceptable Performance of Trace Explosive Detectors, ASTM International, West Conshocken, PA, 2007.
4 G. W. Cook, P. T. LaPuma, G.L. Hook, and B. A. Eckenrode, Using gas chromatography with ion mobility spectrometry to resolve explosive compounds in the presence of interferents, J. Forensic Sci., 2010, 55, 1582-1591.
5 R. Fernández-Maestre, C. S. Harden, R. G. Ewing, C. L. Crawford and H. H. Hill Jr., Chemical standards in ion mobility spectrometry, Analyst, 2010, 135, 1433-1442.
6 L. T. Demoranville, L. Houssiau, and G. Gillen, Behavior and evaluation of tetraalkylammonium bromides as instrument test materials in thermal desorption ion mobility spectrometers, Anal. Chem., 2013, 85(5), 2652-2658.
7 J. Moran, H. McCall, B. Yeager, and S. Bell, Characterization and validation of ion mobility spectrometry in methamphetamine clandestine laboratory remediation, Talanta, 2012, 100, 196-206.
8 ASTM E2677-14, Standard test method for the determination of limit of detection in trace explosive detectors, ASTM International, West Conshocken, PA, 2014.
9 E. Windsor, M. Najarro, A. Bloom, B. Benner Jr., R. Fletcher, R. Lareau, and G. Gillen, Application of inkjet printing technology to produce test materials of 1,3,5-trinitro-1,3,5 triazcyclohexane for trace explosive analysis, Anal. Chem., 82(2), 8519-8524.
10 J. Kozole, J. Tomlinson-Phillips, J. R. Stairs, J. D. Harper, S. R. Lukow, R. T. Lareau, H. Boudries, H. Lai, and C. S. Brauer, Characterizing the gas phase ion chemistry of an ion trap mobility spectrometry based explosive trace detector using a tandem mass spectrometer, Talanta, 2012, 99, 799-810.
11 J. Kozole, J. R. Stairs, I. Cho, J. D. Harper, S. R. Lukow, R. T. Lareau, R. DeBono, and F. Kuja, Interfacing an ion mobility spectrometry based explosive trace detector to a triple quadrupole mass spectrometer, Anal. Chem., 2011, 83, 8596-8603.
12 M. E. Staymates, W. J. Smith, and E. Windsor, Thermal desorption and vapor transport characteristics in an explosive trace detector, Analyst, 2011, 136(19), 3967-3972.
13 M. Najarro, M. E. D. Morris, M. E. Staymates, R. Fletcher, and G. Gillen, Optimized thermal desorption for improved sensitivity in trace explosives detection by ion mobility spectrometry, Analyst, 2012, 137(11), 2614-2622.
14 ISO/IEC Guide 98-3: 2008 Guide to the expression of uncertainty in measurement (GUM) ISO, Geneva, 1993.
15 H. Ku, Notes on the use of propagation of error formulas, J. Research Natl. Bureau of Stds. C. Engineering and Instrumentation, 1966, 70(4), 263-273.
16 B. N. Taylor and C. E. Kuyatt, NIST Technical Note 1297, 1994 Ed. Guidelines for evaluating and expressing the uncertainty of NIST measurement results, NIST, Gaithersburg, MD 20899.
17 R. M. Verkouteren and J. R. Verkouteren, Inkjet metrology: high-accuracy mass measurements of microdroplets produced by a drop-on-demand dispenser, Anal. Chem., 2009, 81(20), 8577-8584.
18 R. M. Verkouteren and J. R. Verkouteren, Inkjet metrology II: resolved effects of ejection frequency, fluidic pressure, and droplet number on reproducible drop-on-demand dispensing, Langmuir, 2011, 27(15), 9644-9653.
19 NIST/SEMATECH e-Handbook of Statistical Methods, http://www.itl.nist.gov/div898/handbook/, 2013.
20 G. A. Eiceman, Z. Karpas, and H. H. Hill, Jr., Ion Mobility Spectrometry, 3rd Ed., CRC Press, Boca Raton, 2014.
21 J. R. Verkouteren, R. M. Verkouteren, and S. Dickinson, Development of inkjet printed materials for use in pilot test of deployed trace explosives detectors: Itemiser DX, NIST Report of Analysis 637-22-11, 2011, NIST, Gaithersburg, MD 20899.